# Quantitative Analysis on Time-series Nodal Voltages in Linear-time Intervals

Zongjie Wang
Department of Electrical and Computer Engineering
Eversource Energy Center
University of Connecticut, Storrs, USA, 06268
zongjie.wang@uconn.edu

## Abstract

*The power flow problem is fundamental to all aspects of modelling, analysis, operation, and control of transmission and distribution systems. In a nutshell, it amounts to solving for the nodal voltages in the nonlinear active- and reactive power balance equations that characterize the steady-states of AC electric networks. Traditional power flow algorithm is focused on the steady operational state under a single snapshot and calculates the corresponding voltage and power distributions for given nodal power injections and network topology. To better capture the temporal characteristics of power injections and system variables with high accuracy, a linear-time interval regarding nodal power injections is first defined in this paper, the norms of nodal voltage derivatives are further analyzed, which is leveraged for simplifying the complexity of solving non-linear dynamic time-varying problems. The voltage monotonicity property has been guaranteed under the proposed linear-time interval. Simulation case studies on IEEE 5-bus and modified 118-bus systems have demonstrated the effectiveness and efficiency of the proposed algorithm.*

## 1. Introduction

Power flow analysis is a fundamental concept in the investigate problems in power system operation and planning [1, 2, 3]. Power flow analysis determines the steady state nodal voltages and branch power flow, based on a specified generating state and transmission network structure [4, 5].

Loads in power systems are always time-varying with the steady-state power system operation focused on a time period. Therefore, it becomes more beneficial to power systems operational security, power quality and economic efficiency if power system problems are analyzed and the dispatch schedules are generated from the perspective of a time period. The idea of considering steady operational states into a time period has been activated for quite a long time, such as, the unit commitment problems at early stage [6, 7] and dynamic optimal power flow in 2000 [8, 9]. The continuation power flow (CPF) algorithm that considers the continuous power over time was first proposed in [10] as an important tool in steady-state voltage stability analysis and has been widely applied into voltage stability margin index [11] and real-time power network applications [12, 13]. However, CPF is under the premise of continuously adding weights on the loads of one node or some nodes, which is focused on the load variations that aims to achieve the critical voltage collapse points, this is not time related and thus CPF also does not characterize the power operational steady-states over a time period. In addition, the quasi-static time-series (QSTS) power flow was proposed and applied mostly in distributed energy resources under distribution systems, and is also used for impact studies of control schemes in different power equipment, such as, smart inverters [14], and voltage regulating devices [15]. Although the QSTS power flow specifically model the discrete controls and run a time-series simulation to capture the time-dependent states of any controllable elements, the requirements for the time-step resolution and the time horizon of QSTS lack a quantitative study in the literature. Specifically, detailed studies regarding the measurements of the errors caused by QSTS power flow including the time-step resolution, input data resolution, and the simulated time horizon are still facing challenges and not yet been well developed.

In addition to that, since the traditional optimal power flow (TOPF) model is focused on a single snapshot, and with the implicit assumption that the OPF solution will satisfy system constraints until the next solution point, it is obvious that the power flow distributions are not well represented for all snapshots between the subsequent solutions in TOPF. Historically, these inaccuracies have been managed by spinning reserves and automatic generation control (AGC) [16, 17]. However, due to the rapid integration

URI: https://hdl.handle.net/10125/102947
978-0-9981331-6-4

of variable renewable energies (VREs) (e.g., wind farms, solar sites) which brings into uncertainty with more fluctuate and unpredictable loading conditions, there is no guarantee that solutions obtained at specific time points will satisfy constraints at non-specified time points, especially for binding constraints [18, 19]. Thus an efficient and accurate OPF algorithm that can guarantee all the involving operational constraints, including the load balance, thermal, and voltage limits, on all the nodes, over all the snapshots under a time horizon, are critical to maintain power system reliability and security. With that being said, a fundamental power flow calculation over a time period with high efficiency and accuracy is of paramount importance to achieve the goal. Specifically, it is necessary to present a time-varying power flow algorithm and to quantitatively analyze the time series nodal voltage properties under the linear time intervals. As a prerequisite of the above, this paper first proposes the concept of linear-time interval, in which the power injections are linear mapping of time. Linear-time interval is a fundamental and important concept through this research, such a linear-time interval actually exists in practical power system planning and operation. Linear-time interval represents the forecasting output level between two consecutive discrete time points during generation scheduling plans. Under a linear-time interval, quantitative properties of the norms of voltage derivatives under rectangular coordinates are analyzed; nodal voltages are theoretically shown to be approximately linear of time which even holds for heavy power variation ranges that are above 100%. Simulation studies under different sizes of IEEE test systems have shown the effectiveness and efficacy of the proposed linear time-varying function. Maximum nodal voltage errors are further validated to show that proposed function carries with high accuracy rate compared with the existing methods in MATPOWER.

## 2. Linear-time intervals

We first assume the beginning time point and ending time point of a time interval $T_l$ are $t_0$, $t_e$ respectively, that is, $T_l \in [t_0, t_e]$. For a time interval $T_l$, if the active power of all nodes (except the slack node) and reactive power of all PQ nodes are linear functions of time *t*, then we define $T_l$ as a linear-time interval.

The defined linear-time interval regarding power injections actually exists in practical power systems.

From engineering perspective, the dispatch center arranges the generation scheduling plans based on load forecasts/equivalent load forecasts with VREs, such as wind/solar power sources. Load forecasts including total and nodal loads are oriented towards discrete time points for a future time period. A straight line segment is achieved by connecting the load forecasts between two consecutive discrete time points, thus the load forecasting output and the corresponding generation schedules for a future time period is a piecewise linear function of time. Figure 1 gives an example of nodal power forecasting output with hourly discrete forecasting time points during day-ahead scheduling, in which the two power outputs could either represent active or reactive power.

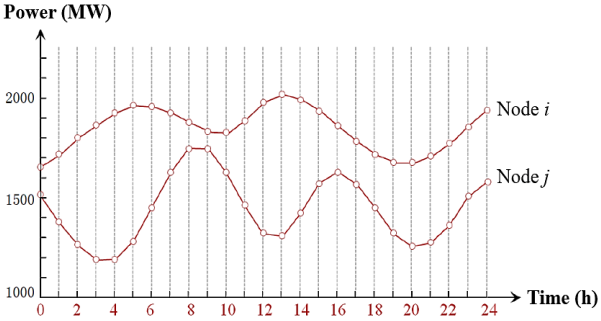


**Figure 1. Nodal forecasting power output during day-ahead scheduling.**

From mathematical perspective, all non-linear time-varying curves can be approximated as piecewise linear functions combined with many linear-time intervals, as the intervals get smaller/the number of intervals gets bigger, the piecewise linear functions gradually match closer to the non-linear time-varying curves. Therefore, linear-time interval is the fundamental approach to solve steady-state non-linear time-varying problems.

The actual load forecasting output is a time-varying curve instead of a piecewise linear function. While making generation scheduling plans for future dispatch time period, dispatch control center only has information about the piecewise linear function of load forecasting. Just like the load forecasting error is inevitable, the error caused from replacing with piecewise linear function is also inevitable.

The proposed linear-time interval discretize a continuous non-linear time-varying problem into several combined linear-time intervals sub-problems, and thus reduces the complexity of finding solutions under non-linear time-varying problems.

If we assume $\Delta T_l$ is the length of the linear-time interval $T_l$ , and is the time difference between any time point *t* and the beginning time point $t_0$ , then

$$\begin{cases} \Delta T_l = t_e - t_0 \\ \Delta t = t - t_0 \end{cases}. \tag{1}$$

$$\begin{cases} P_i(t) = P_i(t_0) + K_{Pi}\Delta t, & (\forall i \notin V\theta\ bus) \\ Q_i(t) = Q_i(t_0) + K_{Qi}\Delta t, & (\forall i \in PQ\ bus) \end{cases}, \quad (2)$$

Thus, for any time point, $t \in T_l$ , the active power of all nodes (except the slack node) and reactive power of all PQ nodes can be represented as follows:

$$\begin{cases} K_{Pi} = \dfrac{1}{\Delta T_l}\Delta P_i \\ K_{Qi} = \dfrac{1}{\Delta T_l}\Delta Q_i \end{cases}. \quad (3)$$

Herein, $\Delta P_i$ and $\Delta Q_i$ are respectively the increments of active and reactive power of node $i$ for linear-time interval $T_l$:

$$\begin{cases} \Delta P_i = P_i(t_e) - P_i(t_0) \\ \Delta Q_i = Q_i(t_e) - Q_i(t_0) \end{cases}. \quad (4)$$

The vector form of (2) is expressed as

$$\begin{cases} \boldsymbol{P}(t) = \boldsymbol{P}(t_0) + \Delta t\boldsymbol{K}_P \\ \boldsymbol{Q}(t) = \boldsymbol{Q}(t_0) + \Delta t\boldsymbol{K}_Q \end{cases}. \quad (5)$$

If

$$y(t) = \begin{bmatrix} \boldsymbol{P}(t) \\ \boldsymbol{Q}(t) \end{bmatrix},\ k = \begin{bmatrix} \boldsymbol{K}_P \\ \boldsymbol{K}_Q \end{bmatrix}, \quad (6)$$

then

$$y(t) = y(t_0) + \Delta t\boldsymbol{k}, \quad (7)$$

where $\boldsymbol{k}$ is the slope vector for linear-time interval $T_l$ and is related to different time units. In this paper, the slope vectors in hour, minute and second units are represented as $\boldsymbol{k}_h, \boldsymbol{k}_m, \boldsymbol{k}_s$, respectively, and they satisfy the following condition:

$$\boldsymbol{k}_h = 60\boldsymbol{k}_m = 3600\boldsymbol{k}_s. \quad (8)$$

Without loss of generality, we choose hourly unit in this paper with the corresponding slope vector $\boldsymbol{k}_h$.

## 3. Nodal voltage derivatives

In rectangular coordinate, the time-varying nodal voltage vector $\boldsymbol{x}(t)$ is

$$\boldsymbol{x}(t) = \begin{bmatrix} \boldsymbol{V}_{re}(t) \\ \boldsymbol{V}_{im}(t) \end{bmatrix}, \quad (9)$$

where $\boldsymbol{V}_{re}(t)$ and $\boldsymbol{V}_{im}(t)$ are the real part and imaginary part of nodal voltage vectors, respectively. Thus the time-varying power equation is expressed as:

$$\boldsymbol{h}(\boldsymbol{x}(t)) = \boldsymbol{y}(t). \quad (10)$$

The corresponding first derivative of nodal voltages is

$$\boldsymbol{J}(t)\boldsymbol{x}^{(1)}(t) = \boldsymbol{k}, \quad (11)$$

where $\boldsymbol{J}(t)$ is the Jacobian matrix shown as follows:

$$\boldsymbol{J}(t) = \frac{\partial}{\partial \boldsymbol{x}}\boldsymbol{h}(\boldsymbol{x}(t)). \quad (12)$$

Since the elements in Jacobian matrix $\boldsymbol{J}(t)$ are linear function of nodal voltages in rectangular coordinates, we get

$$\boldsymbol{J}^{(k)}(t) = \boldsymbol{J}(\boldsymbol{x}^{(k)}(t)),\ (k \geqslant 0). \quad (13)$$

By continuously calculating the derivatives of (11), we get the following $d^{th}$ order of nodal voltage derivative:

$$\boldsymbol{J}(t)\boldsymbol{x}^{(d)}(t) = \boldsymbol{b}_d(t),\ (d \geqslant 1), \quad (14)$$

herein, when $d = 1$:

$$\boldsymbol{b}_1(t) = \boldsymbol{k}; \quad (15)$$

when $d \geqslant 2$:

$$\boldsymbol{b}_d(t) = -\sum_{k=1}^{d-1} C_{d-1}^k \boldsymbol{J}(\boldsymbol{x}^{(k)}(t))\boldsymbol{x}^{(d-k)}(t),\ (d \geqslant 2), \quad (16)$$

where

$$C_{d-1}^k = \frac{(d-1)!}{k!(d-1-k)!}. \quad (17)$$

## 4. Time-varying nodal voltage properties in linear-time intervals

### 4.1. Matrix and vector norms

Norms are compatible, if

$$\boldsymbol{m}\boldsymbol{v} = \boldsymbol{b}, \quad (18)$$

then

$$\|\boldsymbol{m}\boldsymbol{v}\|_p = \|\boldsymbol{b}\|_p, \quad (19)$$

and satisfies

$$\|\boldsymbol{m}\|_p\|\boldsymbol{v}\|_p \geqslant \|\boldsymbol{b}\|_p, \quad (20)$$

where $\boldsymbol{m}$ is matrix, $\boldsymbol{v}$ and $\boldsymbol{b}$ are the vectors that are compatible with matrix $\boldsymbol{m}$.

Norms also have equivalence property, for $p$-norms when $p = 1, 2, \infty$, if one of the norms follows the corresponding equality/inequality, so do the other two norms.

### 4.2. Norm of nodal voltage derivative vectors

The condition number of Jacobian matrix $\boldsymbol{J}(t)$ is

$$\rho_t = \left\|\boldsymbol{J}^{-1}(t)\right\|_p \|\boldsymbol{J}(t)\|_p,\ (p = 1, 2, \infty). \tag{21}$$

The condition number $\rho_t$ can be corrected for a given proper coefficient $\alpha_t \in (0, 1)$:

$$\tilde{\rho}_t = \alpha_t \rho_t \leqslant \rho_t, \tag{22}$$

thus the inequality condition shown in the proposition 2 is further transformed into the following approximate equality:

$$\left\|\boldsymbol{x}^{(d)}(t)\right\| \approx (2d-3)!!\tilde{\rho}_t^{d-1}\left\|\boldsymbol{x}^{(1)}(t)\right\|^d,\ (d \geqslant 2). \tag{23}$$

### 4.3. Time-varying nodal voltage properties

**Property 1.** *For a linear-time interval, the nodal voltage function has approximate linearity with respect to time.*

The corresponding discussions are as follows.

According to the Taylor series expansion, the following time-varying nodal voltages in a linear-time interval are expressed as

$$\boldsymbol{x}(t) = \boldsymbol{x}(t_0) + \sum_{k=1} \frac{1}{k!}\Delta^k t \boldsymbol{x}^{(k)}(t_0), \tag{24}$$

In addition, we have

$$\begin{cases} \left\|\boldsymbol{x}^{(2)}(t)\right\| \approx \tilde{\rho}_t \left\|\boldsymbol{x}^{(1)}(t)\right\|^2 \\ \left\|\boldsymbol{x}^{(3)}(t)\right\| \approx 3\tilde{\rho}_t^2 \left\|\boldsymbol{x}^{(1)}(t)\right\|^3 \end{cases}. \tag{25}$$

The order of magnitude for $\left\|\boldsymbol{x}^{(1)}(t)\right\|$ is within $10^{-1}$, the order of magnitude for $\tilde{\rho}_t$ is $10^0$, thus the order of magnitude for $\left\|\boldsymbol{x}^{(2)}(t)\right\|$ is within $10^{-2}$; and it will be much smaller for $\left\|\boldsymbol{x}^{(3)}(t)\right\|$. Under the condition of $\Delta t < 1$, if the $2^{nd}$ and the above orders of derivative for (24) is approximated to be zero, then the nodal voltages are approximated as linear functions with respect to time, that is,

$$\boldsymbol{x}(t) = \boldsymbol{x}(t_0) + \Delta t \boldsymbol{x}^{(1)}(t_0). \tag{26}$$

(26) is called linear time-varying function with the corresponding norm of absolute error given by

$$\|\boldsymbol{R}_1(t)\| = \frac{1}{2}\Delta^2 t \left\|\boldsymbol{x}^{(1)}(t_0 + \eta\Delta t)\right\|,\ (0 < \eta < 1). \tag{27}$$

The above absolute error is characterized through the $2^{nd}$-order of derivative, the corresponding order of magnitude is within $10^{-2}$. Since the orders of magnitude for real part and imaginary part of nodal voltages are $10^0$, the order of magnitude for relative voltage error is also within $10^{-2}$. This indicates that the nodal voltage function with respect to time has approximate linearity in a linear-time interval $T_l$.

### 4.4. Numerical simulations of time-varying nodal voltage properties

Based on MATPOWER, the IEEE 5-bus system is simulated to numerically evaluate the time-varying nodal voltage properties in a linear-time interval $T_l$. The corresponding network topology is shown in Figure 2, wherein bus 5 is a slack bus, bus 1 is a *PV* bus with a voltage magnitude of 1.05 *p.u.*, the rest of the buses are *PQ* buses.

The linear-time interval is considered as 1h. The active power output from *PQ* buses and *PV* bus are shown in Figure 3(a). Similarly, the reactive power output from *PQ* buses are shown in Figure 3(b).

To better illustrate the effectiveness of the proposed properties, we intentionally design some heavy node power variation ranges to make sure that the total power variation range is above 100%. In addition, to avoid the same trends from nodal power/total power (e.g., either simultaneously increasing or decreasing), we also randomly design different trends of nodal active and reactive power, respectively (e.g., if the active power on node *i* increases, then the reactive power on node *i* decreases).

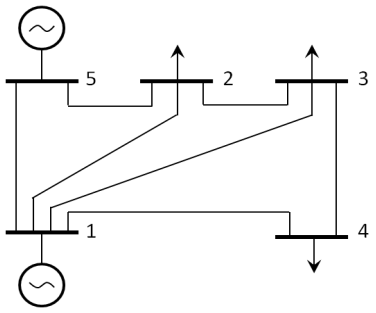


**Figure 2. IEEE 5-bus test system.**

The simulation results of time-varying nodal voltage function in a linear-time interval $T_l$ are shown in Figure 4. The **"o"** marker represents the actual nodal voltage values calculated from power flow in MATPOWER, the straight line between the two consecutive time points represents the computational values from linear time-varying function in (26). We can see that, the corresponding curves of real part and imaginary part of

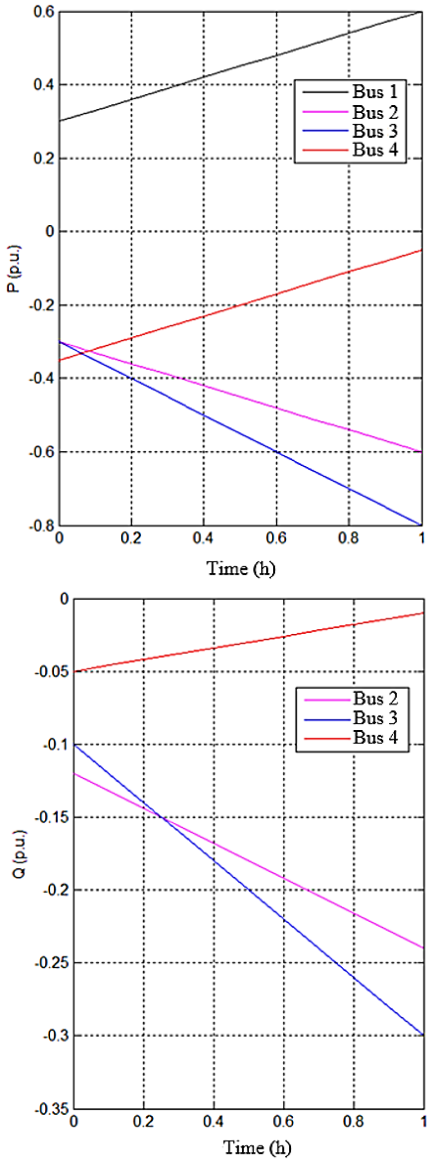


**Figure 3. Power Output within a given linear-time interval.**

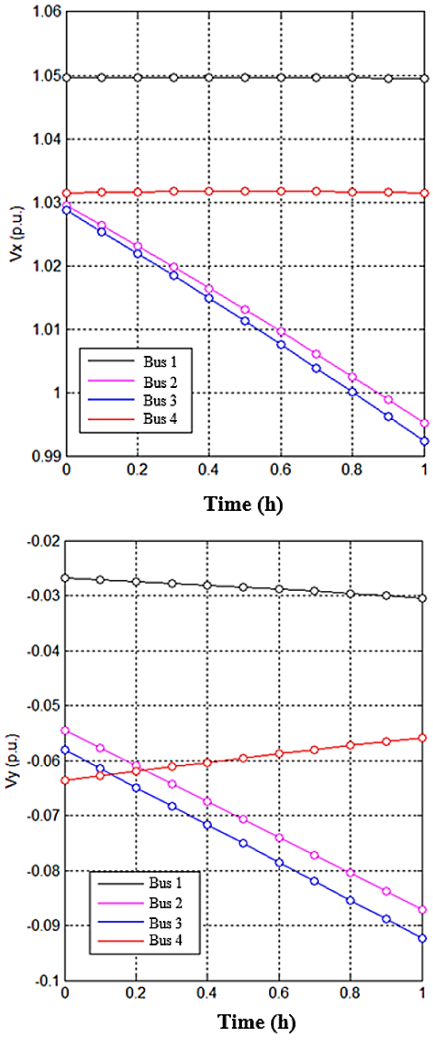


**Figure 4. Computational results of linear time-varying function.**

nodal voltages in a linear-time interval are extremely close to a straight line, thus can be approximated as linearity. This observation aligns well with the proposed property 1.

Relative errors between the computational results from linear time-varying function (shown in Figure 4) and the corresponding existing methods calculated in MATPOWER (also shown in Figure 4) are further presented in Figure 5. We can see that the orders of magnitude for both real part and imaginary part of nodal voltages errors are within $10^{-2}$, which coincide with the theoretical analysis achieved from (27). Simulation results demonstrate that under a linear-time interval $T_l$, nodal voltage function is satisfied to be approximated as a linear time-varying function, as shown in (26).

## 5. Numerical simulations

In this section, a modified IEEE 118-bus system is simulated, where 20 wind generators and 10 solar generators are added. Assume that there is no curtailment of renewable generation, then the total power generation from VREs is 30% of the total demand, with the wind power generation of being 60% of the total VREs power output. Thus a power system with high penetrations of VREs is presented. The corresponding network topology is shown in Figure 6, where bus 69 is a slack bus.

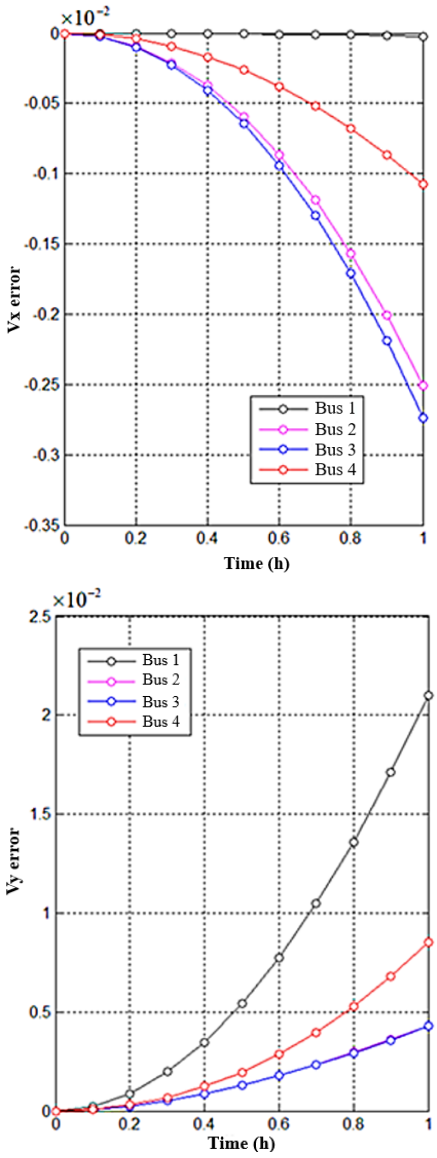


**Figure 5. Relative errors of linear time-varying function.**

The total time period is considered as 24h, which is designed to coherent with the future dispatch period while making day-ahead generation scheduling plans. 25 discrete time points $t_l$ partition the entire time period into 24 linear-time intervals. In addition, to better evaluate and demonstrate the proposed properties, each linear-time interval (1h) is further partitioned with 11 equidistant discrete time points.

Similar to the previous simulations, to better illustrate the effectiveness of the proposed properties, we intentionally design some heavy nodal power variation ranges so that the total power variation range is above 100%. In addition, to avoid the same trends from

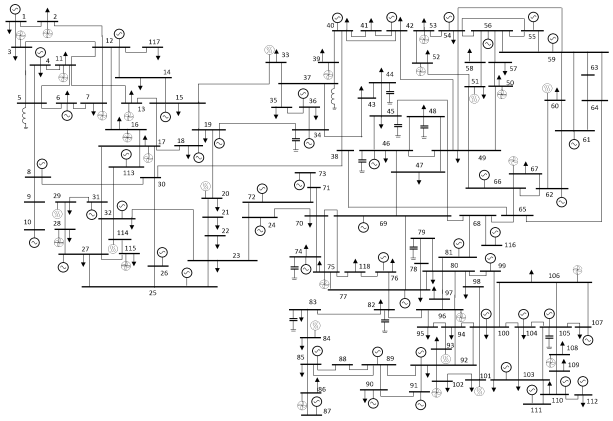

**Figure 6. A modified IEEE 118-bus system.**

nodal power/total power (e.g., either simultaneously increasing or decreasing), we also randomly design different trends of nodal active and reactive power, respectively (e.g., if the active power on node $i$ increases, then the reactive power on node $i$ decreases). The total active and reactive power curves are shown in Figure 7.

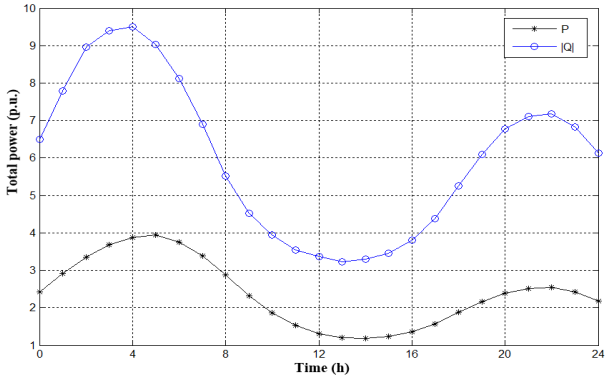


**Figure 7. Total power curves within 24h.**

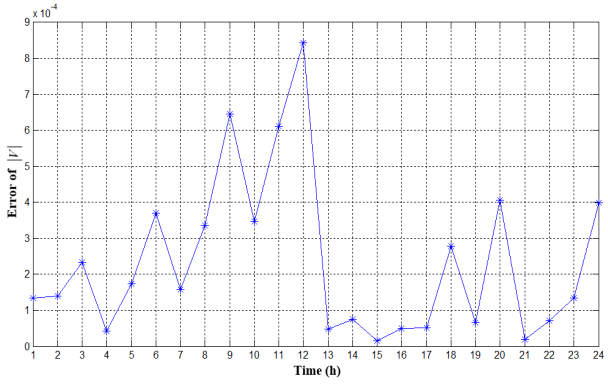


**Figure 8. Maximum voltage errors for each linear-time interval within 24h.**

Nodal voltage magnitudes are calculated at any snapshot over the 24 linear-time intervals. In other words, take node *i* for example, since there are 11 equidistant time points in each linear-time interval, the voltage magnitudes on node *i* are calculated 241 times in the 24h time period. Thus the voltage errors on each node between computational values and the corresponding power flow solutions (calculated in MATPOWER) at any time point in these 24 linear-time intervals are then achieved. Compared with the existing methods in MATPOWER, we respectively record the maximum voltage error under each linear-time interval, with the results shown in Figure 8. Note that the maximum voltage error under each linear-time interval is selected among voltage errors of all the nodes from 11 equidistant time points, that is $118 \times 11 = 1298$.

Figure 8 shows that, the maximum nodal voltage error of all the maximum voltage errors through 24 linear-time intervals occurs on the $12^{th}$ linear-time interval over the entire time period, with the corresponding error being $8.4 \times 10^{-4}$. The minimum nodal voltage error of the maximum voltage errors through 24 linear-time intervals occurs on the $15^{th}$ linear-time interval over the entire time period, with the corresponding error being $1.4 \times 10^{-5}$.

We can see from the above results that, since the maximum voltage error selected among all the nodes in 11 equidistant time points in all the 24 linear-time intervals ($118 \times 241 = 28438$) is $8.4 \times 10^{-4}$, the order of magnitudes for all the nodes are guaranteed to be within $10^{-2}$, which further demonstrates the time-varying power flow is with high computational accuracy.

## 6. Conclusions

Power flow analysis is an important prerequisite in power systems especially when it comes to economic dispatch/optimal power flow. Traditional optimal power flow describes the system performance only in a single specified time point while the resulting decisions are applied to an entire time period. Since power system balanced steady operation state varies over time, it is necessary to explore the properties regarding state/control variables to ensure system's stability and security. Starting from this point of view, the conclusions of this paper are shown as a prerequisite of the above.

(i) A linear-time interval in which the nodal power injections are linear functions of time is proposed in this paper. Theoretically, linear-time interval is the fundamental approach to solve steady-state non-linear time-varying problems. Practically, linear-time interval exists in real power systems to determine the generation scheduling plans based on load forecasts. Thus linear-time interval is the key to discretize and linearize the non-linear time-varying problems.

(ii) For a linear-time interval, the nodal voltage properties have been quantitatively studied. The nodal voltage magnitudes are also shown with approximate linear functions of time.

(iii) The linear time-varying function is proposed within a high promising computational accuracy. Simulation case studies have further demonstrated the effectiveness and the efficiency of the proposed function.

## 7. Future work

Based on the time-varying nodal voltage properties and the proposed algorithm in this paper, our future work will be focused on optimal power flow towards a time period and the corresponding applications into economic dispatch systems including day-ahead scheduling and real-time dispatch, typically in large-scale actual/synthetic power systems with high penetrations of VREs.

## References


[1] J. Carpentier, "Contribution to the economic dispatch problem," *Bulletin de la Societe Francoise des Electriciens*, vol. 3, no. 8, pp. 431–447, 1962.

[2] D. K. Molzahn, I. A. Hiskens, *et al.*, "A survey of relaxations and approximations of the power flow equations," *Foundations and Trends® in Electric Energy Systems*, vol. 4, no. 1-2, pp. 1–221, 2019.

[3] R. Bent, G. L. Toole, and A. Berscheid, "Transmission network expansion planning with complex power flow models," *IEEE Transactions on Power Systems*, vol. 27, no. 2, pp. 904–912, 2011.

[4] Z. Wang and C. L. Anderson, "A progressive period optimal power flow for systems with high penetration of variable renewable energy sources," *Energies*, vol. 14, no. 10, p. 2815, 2021.

[5] P. Kumar and A. K. Singh, "Load flow analysis with wind farms," in *Handbook of Distributed Generation*, pp. 149–170, Springer, 2017.

[6] R. R. Shoults, S. K. Chang, S. Helmick, and W. M. Grady, "A practical approach to unit commitment, economic dispatch and savings allocation for multiple-area pool operation with import/export constraints," *IEEE Transactions on Power Apparatus and Systems*, no. 2, pp. 625–635, 1980.

[7] G. Guo, L. Zephyr, J. Morillo, Z. Wang, and C. L. Anderson, "Chance constrained unit commitment approximation under stochastic wind energy," *Computers & Operations Research*, vol. 134, p. 105398, 2021.

[8] N. Alguacil and A. Conejo, "Multiperiod optimal power flow using benders decomposition," *IEEE Transactions on power systems*, vol. 15, no. 1, pp. 196–201, 2000.

[9] Z. Wang, G. Guo, and C. L. Anderson, "Simulation case studies on period optimal power flow," in *2019 Winter Simulation Conference (WSC)*, pp. 3669–3680, IEEE, 2019.

[10] S. R., *Practical Bifurcation and Stability Analysis from Equilibrium to Chaos*. Springer Verlag, 1994.

[11] L. Van Dai, N. Minh Khoa, and C. Le Quyen, "An innovatory method based on continuation power flow to analyze power system voltage stability with distributed generation penetration," *Complexity*, vol. 2020, 2020.

[12] A. J. Flueck and J. R. Dondeti, "A new continuation power flow tool for investigating the nonlinear effects of transmission branch parameter variations," *IEEE Transactions on Power Systems*, vol. 15, no. 1, pp. 223–227, 2000.

[13] K. Alzaareer, M. Saad, H. Mehrjerdi, C. Z. El-Bayeh, D. Asber, and S. Lefebvre, "A new sensitivity approach for preventive control selection in real-time voltage stability assessment," *International Journal of Electrical Power & Energy Systems*, vol. 122, p. 106212, 2020.

[14] M. Baggu, R. Ayyanar, and D. Narang, "Feeder model validation and simulation for high-penetration photovoltaic deployment in the arizona public service system," in *2014 IEEE 40th Photovoltaic Specialist Conference (PVSC)*, pp. 2088–2093, IEEE, 2014.

[15] J. E. Quiroz, M. J. Reno, and R. J. Broderick, "Time series simulation of voltage regulation device control modes," in *2013 IEEE 39th Photovoltaic Specialists Conference (PVSC)*, pp. 1700–1705, IEEE, 2013.

[16] M. V. Liu, B. Yuan, Z. Wang, J. A. Sward, K. M. Zhang, and C. L. Anderson, "An open source representation for the nys electric grid to support power grid and market transition studies," *IEEE Transactions on Power Systems*, 2022.

[17] A. Younesi, H. Shayeghi, Z. Wang, P. Siano, A. Mehrizi-Sani, and A. Safari, "Trends in modern power systems resilience: State-of-the-art review," *Renewable and Sustainable Energy Reviews*, vol. 162, p. 112397, 2022.

[18] L. Zephyr, G. Guo, Z. Wang, and J. Morillo, "Approximate chance-constrained unit commitment under wind energy penetration," in *Proceedings of the 55th Hawaii International Conference on System Sciences*, 2022.

[19] Z. Wang and Z. Guo, "Toward a characteristic optimal power flow model for temporal constraints," in *2017 IEEE Transportation Electrification Conference and Expo, Asia-Pacific (ITEC Asia-Pacific)*, pp. 1–6, IEEE, 2017.